COMMUNICATION SCIENCES AND ENGINEERING

XXV. STATISTICAL COMMUNICATION THEORY*

Academic and Research Staff

Prof. Y. W. Lee	Prof. J. D. Bruce	Prof. D. E. Nelsen
Prof. A. G. Bose	Prof. A. V. Oppenheim	G. Gambardella

Graduate Students

T. Huang	R. W. Schafer	J. L. Walker
V. Nedzelnitsky	J. E. Schindall	J. J. Wawzonek
L. R. Poulo	F. P. Tuhy	C. J. Weinstein
A. E. Rolland		D. H. Wolaver

RESEARCH OBJECTIVES

1. Investigation of Switching Systems

There is an increasing need for systems that handle analog signals but operate in a switching mode. Such switching systems offer efficiency, size, and weight advantages over conventional analog systems. The analysis of these systems, however, is complicated by the fact that they often take the form of closed-loop nonlinear systems. Analysis and synthesis procedures are necessary in order to optimally design these systems and to determine their ultimate performance capabilities.

The principal efforts during the past three years have been devoted to static analysis. An exact static analysis has been achieved by A. G. Bose[1] and has provided useful design guidelines. The noise analysis has been carried out for the special case of a tunnel-diode switching circuit by D. E. Nelsen.[2]

Work is now under way to determine the dynamic performance of these systems. During the coming year it is hoped that a better understanding of the transient response and spectrum properties will be obtained. We also plan to extend the noise studies to other switching devices and circuits. An eventual goal in this project is to obtain noise models for switching devices in much the same way as we have done for noise models of devices operating in the linear mode.

2. Modulation Noise in Tape Recording

Modulation noise in tape recording is a wide-band noise whose intensity increases with increasing recorded signal on the tape. The phenomenon has been well documented, but adequate explanations and models are not available. We hope that a proper model will aid in the development of lower noise tapes.

Extensive experiments have been made to isolate noises of other origins (electrical and mechanical) from the modulation noise. The spectral properties of modulation noise have been measured under varying conditions of recording and playback. A theoretical model has been derived which relates the modulation noise to particle interaction on the tape.

---

*This work was supported by the Joint Services Electronics Programs (U.S. Army, U.S. Navy, and U.S. Air Force) under Contract DA 36-039-AMC-03200(E), the National Aeronautics and Space Administration (Grant NsG-496), and the National Science Foundation (Grant GK-835).

Further experiments are necessary to correlate the predictions indicated by the model with physical observations on tape noise. Recommendations for reduction of the noise will be made after verification of the noise model.

3. Recording and Reproduction of Sound

The design of loudspeakers and of recording techniques has remained a controversial and poorly understood area for decades. Standards committees have not been able to agree upon an acceptable design criterion or measurement technique for evaluation of the commom loudspeaker. This subject is complicated by the fact that objective criteria are desired for transducers whose ultimate use involves subjective evalution.

A design criterion has been developed which makes use of Green's function to produce recordings of sound as they would be heard if reproduced in a room through an ideal transducer. A computer-aided design program has yielded the design of a practical transducer whose performance is subjectively indistinguishable from that of the ideal transducer.[3]

Efforts will now be directed toward problems in the recording of sound. The effects of the normal mode structure of the recording environment will be investigated and the constraints that this structure imposes upon the techniques and procedures of recording will be determined.

4. Optimum Quantization

Exact expressions for the quantization error as a function of the quantizer parameters, the error-weighting function, and the amplitude probability density of the quantizer-input signal have been derived by J. D. Bruce.[4] An algorithm based on these expressions, which permits the determination of the specific values of quantizer parameters that minimize the quantization error (with respect to some particular error-weighting function) has been developed. The error expressions and the algorithm have been extended to the case in which the quantizer-input signal is a message signal contaminated by a noise signal.

During the past year studies have been concentrated in two particular areas.

a. Subjective evaluation of speech quantizer levels is small and there are requirements of high intelligibility and naturalness.

b. Theoretical investigation of optimum quantizers for quantizer-input signals that are message signals contaminated by noise.

Results have been obtained in each of these areas and are being reported.[5,6] In particular, it is now possible to characterize a quantizer by certain of its properties so as to be able to say whether or not it is desirable for use in a speech-transmission system. Also, these same properties classify the type of distortion that the quantizer will introduce. With respect to the second area, results have been obtained for the case in which the message signal is discrete. These results are identical to those obtained from the ideal observer point of view in classical decision theory.

Studies in both of these areas will continue during the coming year.

5. Localization of Acoustical Phenomena

For some time, there has been evidence to indicate that the pinna (external ear) plays a primary role in the localization of acoustical phenomena. It is proposed that this role be studied in the forthcoming year with a view toward modeling the external ear and simulating its role in localization.

6. Superposition in a Class of Nonlinear Systems

In 1964, a new characterization of nonlinear systems was developed, and its application to problems in nonlinear filtering was suggested by A. V. Oppenheim.[7] This approach to nonlinear filtering represented a generalization of the linear filtering problem and appeared to be particularly suited to the nonlinear separation of signals that have been nonadditively combinded.

Specific cases of interest, at present, are in the application of this technique to the separation of convolved signals and the separation of multiplied signals. The need for such techniques arises, for example, in the processing of signals after transmission over multipath and fading channels, the removal of echoes from recorded speech and music, and the analysis and bandwidth reduction of speech. It also appears, at present, that the ability to apply these techniques to speech and music suggest some fundamentally new means for modifying their characteristics and for preprocessing before recording or transmission to enhance their quality.

Primary empahsis during the past year has been directed toward the separation of convolved signals. The filter was simultated on a digital computer and initial studies were carried out with both artificially generated waveforms and speech. A preliminary investigation of the effect of additive noise on the processing was initiated.

Work will continue on a study of the separation of convolved signals. In particular, speech with artificially generated echoes will be processed to recover the original speech. Uncorrupted speech will also be processed in an attempt to separate the glottal waveform and the impulse response of the vocal tract.

Attention will also be directed toward the extraction of the low-frequency envelope from music and the processing of waveforms that have been subject to low-frequency fading.

7. Wiener Theory of Nonlinear Systems

The study of this theory was initiated at the Research Laboratory of Electronics in 1949. Many doctoral theses and technical reports have been written on the subject by members of this group. The latest doctoral thesis on the Wiener nonlinear theory was written by R. B. Parente.[8] It contains the first solution of the dynamic stability problem of a magnetic suspension device associated with inertial guidance systems. Present work is directed toward other applications, and the relationship between differential equation representation and functional representation of nonlinear systems.

Y. W. Lee

References

1. A. G. Bose, "A Two-State Modulation System," WESCON, Section 7.1, San Francisco, August 20-23, 1963.
2. D. E. Nelsen, "Statistics of Switching-Time Jitter for a Tunnel Diode Threshold-Crossing Detector," Sc.D. Thesis, Department of Electrical Engineering, M.I.T., June 1966.
3. A. G. Bose, "Relative Effects of Normal Mode Structure of Loudspeakers and Rooms on the Reproduction of Sound," a paper presented at the Sixty-eighth Meeting of the Acoustical Society of America, October 1964.
4. J. D. Bruce, "Optimum Quantization," Technical Report 429, Research Laboratory of Electronics, Massachusetts Institute of Technology, Cambridge, Massachusetts, March 1, 1965.

5. R. W. Koralek, "Speech Quantization Studies," S.B. Thesis, Department of Electrical Engineering, M.I.T., May 1966.

6. J. D. Bruce, "Fixed Representation-Value Quantization of a Discrete Message Signal Plus Noise," to be published.

7. A. V. Oppenheim, "Superposition in a Class of Nonlinear Systems," 1964 IEEE International Convention Record, Part 1, pp. 171-177.

8. R. B. Parente, "Functional Aanlysis of Systems Characterized by Nonlinear Differential Equations," Technical Report 444, Research Laboratory of Electronics, Massachusetts Institute of Technology, July 15, 1966.

A. TRANSFER FUNCTIONS FOR A TWO-STATE MODULATION SYSTEM

1. Introduction

Bose[1,2] has described the simple two-state modulation system diagrammed in Fig. XXV-1 and has demonstrated that the average of the output switching waveform is approximately equal to the negative of the input voltage for fixed values of input signal. The system has application as an efficient switching amplifier, or can operate as a voltage regulator by having the input fixed at a reference voltage and powering the output switching element from the voltage that is to be regulated.

In this report, transfer functions for the modulator are derived for fixed- and ramp-input waveforms. Other aspects of modulator operation are being explored; this work will not be reported here.

2. Transfer Function, Static Input

First, consider the modulator of Fig. XXV-1 with zero delay, and denote the fixed input x_o. It is expedient to visualize the averaging of the two-state output waveform y(t) as taking place in two stages. This is diagrammed (with representative waveforms) in Fig. XXV-2. The two-state waveform y(t) is first passed through a lowpass RC network, with the same time constant as the RC network appearing within the modulator feedback loop. The intermediate signal, $y_i(t)$, which results – identical to the modulator feedback signal f(t) – is then passed through an ideal lowpass filter to yield output $\overline{y}$. Of course, y(t) could just as well be passed directly through the ideal lowpass filter to yield the same $\overline{y}$ as does the two-stage filtering process; however, the modulator error is graphically evident by examination of the intermediate waveform $y_i(t)$.

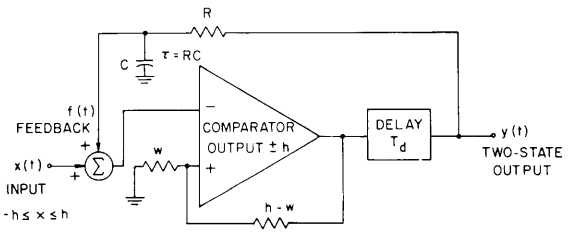

Fig. XXV-1. Two-state modulation system.

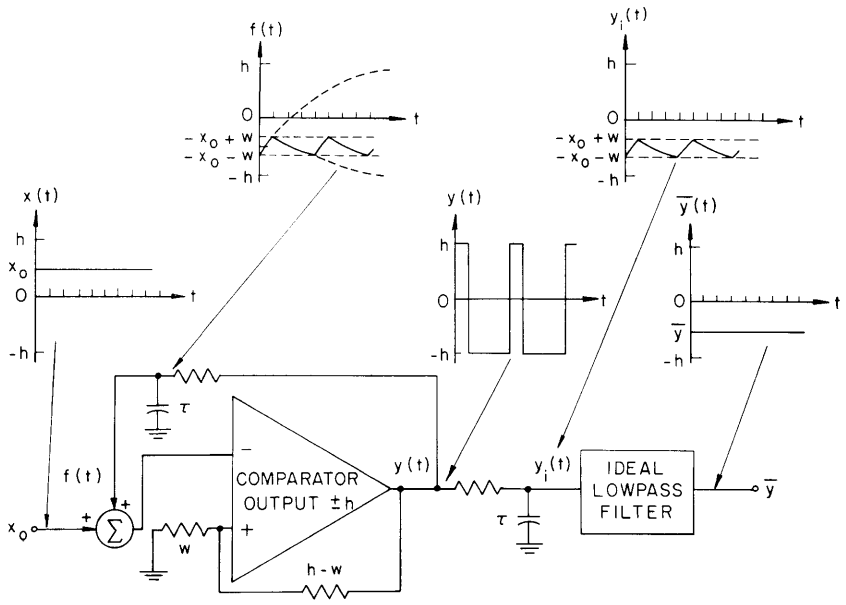

Fig. XXV-2. Modulator waveforms with two-stage output filter (zero-delay).

Since $y_i(t)$ is identical to f(t), the operation of the modulator loop contrains it to vary between $-x_o - w$ and $-x_o + w$ in an exponential manner. This is shown in Fig. XXV-2. The desired output, $-x_o$, is the midpoint value of $y_i(t)$. The ideal lowpass filter yields output $\bar{y}$ as the average value of $y_i(t)$. Because of the unequal curvature associated with the charge and discharge portions of the waveform $y_i(t)$, the average is equal to the midpoint only for $x_o = 0$. In fact, it is apparent that the discrepancy between average and midpoint (the modulator error) increases as $|x_o|$ and as w (the half-width of the exponential window) increase and acts to produce a modulator gain or transfer function slightly greater than unity.

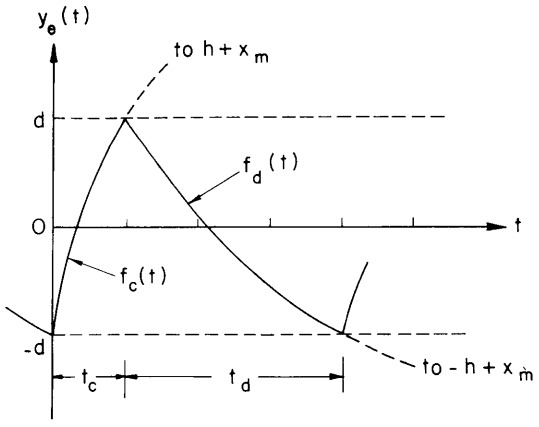

Fig. XXV-3. Exponential-error waveform.

Consider an exponential waveform charging and discharging toward h and -h between limits $-x_m + d$ and $-x_m - d$, where $-x_m$ is the midpoint of the exponential window, and d is the half-width of the window. The object is to derive an expression for the average value of this waveform in terms of its midpoint value and its half-width. To avoid masking

the output error, consider subtracting the midpoint value $-x_m$ from the exponential waveform. The resulting waveform $y_e(t)$ has midpoint zero and varies exponentially between d and -d as sketched in Fig. XXV-3.

The average of $y_e(t)$ is precisely $\overline{y} - (-x_m)$. During the charge portion of the cycle,

$$f_c(t) = (h+x_m) + (-h-x_m-d)\, e^{-t/\tau}. \tag{1}$$

So

$$f_c(t_c) = d = h + x_m + (-h-x_m-d)\, e^{-t_c/\tau}, \tag{2}$$

and

$$t_c = \tau \ln \frac{h + x_m + d}{h + x_m - d}. \tag{3}$$

From (1) and (3),

$$\int_0^{t_c} f_c(t)\, dt = \tau \left[(h+x_m) \ln \left(\frac{h + x_m + d}{h + x_m - d} \right) - 2d \right]. \tag{4}$$

Similarly, for the discharge portion of the cycle,

$$\int_{t_c}^{t_c+t_d} f_d(t)\, dt = -\tau \left[(h-x_m) \ln \left(\frac{h - x_m + d}{h - x_m - d} \right) - 2d \right]. \tag{5}$$

The average over a cycle is given by

$$\frac{1}{t_c + t_c} \int_0^{t_c+t_d} y_e(t)\, dt = \frac{(h+x_m) \ln \frac{h + x_m + d}{h + x_m - d} - (h-x_m) \ln \frac{h - x_m + d}{h - x_m - d}}{\ln \frac{h + x_m + d}{h + x_m - d} + \ln \frac{h - x_m + d}{h - x_m - d}}. \tag{6}$$

Expanding, since $\ln \left[\frac{a+\epsilon}{a-\epsilon} \right] = 2 \left[\frac{\epsilon}{a} + \frac{1}{3} \left(\frac{\epsilon}{a} \right)^3 + \frac{1}{5} \left(\frac{\epsilon}{a} \right)^5 + \ldots \right]$ for $\left| \frac{\epsilon}{a} \right| < 1$, we have

$$\frac{1}{t_c + t_d} \int_0^{t_c+t_d} y_e(t)\, dt = \frac{(h+x_m)\, 2 \left[\frac{d}{h+x_m} + \frac{1}{3} \left(\frac{d}{h+x_m} \right)^3 + \ldots \right] - (h-x_m)\, 2 \left[\frac{d}{h-x_m} + \left(\frac{d}{h-x_m} \right)^3 + \ldots \right]}{2 \left[\frac{d}{h+x_m} + \frac{1}{3} \left(\frac{d}{h+x_m} \right)^3 + \ldots \right] + 2 \left[\frac{d}{h-x_m} + \frac{1}{3} \left(\frac{d}{h-x_m} \right)^3 + \ldots \right]}. \tag{7}$$

Combining terms, to second order we obtain

$$\overline{y} = -x_m \left[1 + \frac{2}{3} \frac{\left(\frac{d}{h}\right)^2}{1 - \left(\frac{x_m}{h}\right)^2} \right] \tag{9}$$

which is the desired transfer function. The result of (9) is under the assumption that $\frac{d}{h \pm x_m} \ll 1$, in that terms of the order of $\left[\frac{d}{h \pm x_m}\right]^4$ have been neglected. The "excess-gain" error term is of order $\left(\frac{d}{h}\right)^2$ and contains a nonlinearity of the form $\left[1 - \left(\frac{x_m}{h}\right)^2\right]$.

For the case of static input and zero delay, the exponential window waveform $y_i(t)$ has midpoint $-x_o$ and half-width w. For this case, then, (9) leads to

$$\overline{y} = -x_o \left[1 + \frac{2}{3} \frac{\left(\frac{w}{h}\right)^2}{1 - \left(\frac{x_o}{h}\right)^2} \right]. \tag{10}$$

Now the effect of nonzero delay in the modulator loop will be considered. Because of the delay, the output does not change until T_d seconds after the feedback waveform has reached $-x_o + w$ or $-x_o - w$. During this time, the feedback waveform and the intermediate waveform $y_i(t)$ overshoot. The effect of delay on $y_i(t)$ is to enlarge the

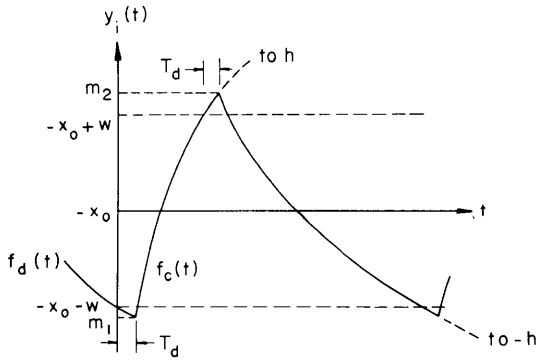

Fig. XXV-4. Intermediate waveform, static input.

exponential window and to displace its midpoint from $-x_o$. This is diagrammed in Fig. XXV-4. Notice that the delay-induced overshoot is more pronounced on the steeper of the two exponential segments, tending to displace the midpoint of the waveform toward the more distant asymptote and thus decrease the magnitude of the modulator gain. From Fig. XXV-4,

$$f_d(t) = -h + (h - x_o - w)\, e^{-t/\tau}, \tag{11}$$

so

$$m_1 = -h + (h - x_o - w)\, e^{-T_d/\tau}. \tag{12}$$

Similarly,

$$m_2 = h + (-h - x_o + w)\, e^{-T_d/\tau}. \tag{13}$$

The midpoint of the exponential window, $-x_m$, is given by

$$-x_m = \frac{m_1 + m_2}{2} = -x_o\, e^{-T_d/\tau}. \tag{14}$$

The half-width of the exponential window, d, is given by

$$d = \frac{m_2 - m_1}{2} = h\left(1 - e^{-T_d/\tau}\right) + w\, e^{-T_d/\tau}. \tag{15}$$

Substituting the delay-altered values of midpoint and half-width from (14) and (15) in Eq. 9 gives

$$\overline{y} = -x_o\, e^{-T_d/\tau}\left\{1 + \frac{2}{3}\,\frac{\left[\left(1 - e^{-T_d/\tau}\right) + \frac{w}{h}\, e^{-T_d/\tau}\right]^2}{1 - \left[\frac{x_o e^{-T_d/\tau}}{h}\right]^2}\right\}. \tag{16}$$

The modulator gain is reduced by a factor of $e^{-T_d/\tau}$ from the zero-delay case, while the nonlinearity and parameter dependence of the result, introduced by the second term in brackets, are increased. Under the assumption that $\frac{T_d}{\tau} \ll 1$, (16) can be written

$$\overline{y} = -x_o\left(1 - \frac{T_d}{\tau}\right)\left[1 + \frac{\left(\frac{T_d}{\tau} + \frac{w}{h}\right)^2}{1 - \left(\frac{x_o}{h}\right)^2}\right]. \tag{17}$$

And, for use of the modulator as a symmetric regulator, (17) predicts

$$\frac{dy}{dh} = 2\,\frac{x_o}{h}\,\frac{\left(\frac{T_d}{\tau} + \frac{w}{h}\right)\left(\frac{x_o^2}{h^2}\,\frac{T_d}{\tau} + \frac{w}{h}\right)}{\left(1 - \frac{x_o^2}{h^2}\right)^2}. \tag{18}$$

3. Dynamic Transfer Function, Ramp Input

An explicit expression for the modulator transfer function with arbitrary dynamic input waveforms cannot be obtained. The problem arises because the modulator switches at time t_s in such a manner that the exponential feedback waveform added to the input signal equals w or -w. This produces an implicit transcendental equation for t_s which admits an explicit solution for t_s only when the input signal is a constant.

A useful approach is to select a particular input waveform appropriate for characterizing the modulator behavior, and seek an approximate solution for this excitation. For a linear system the sinusoidal response provides an effective characterization. In nonlinear systems such as the two-state modulator, however, the sinusoidal response is difficult to express (it is a function of the amplitude and DC level of the input, as well as its frequency) and provides no general information about the system (since superposition does not apply).

The main effect of a dynamic input on modulator operation is that the modulator must track or "keep up" with the time rate of change of the input waveform. This time rate of change, or slope, is characterized by a ramp waveform. With this motivation, characterizing the dynamic response of the modulator by its ramp response leads to an unexpected bonus: although the equations describing the transfer function are transcendental, they can be manipulated to yield an accurate and explicit solution for the particular case of a ramp input. It should be noted that many waveforms can be adequately modeled as a series of ramp segments, each segment being one modulator switching period long.

Derivation of the modulator transfer function with a ramp input is facilitated by characterizing the ramp as altering the effective width and midpoint of the exponential window function $y_i(t)$. Because the modulator operation is asynchronous, one cannot specify or predict "charging" or "discharging" operation of the modulator at any particular instant of time. The desired transfer function will first be obtained by assuming input mean x_o to take place at the center of a modulator charge cycle to give $t_c(x_o) = t_{co}$; then assuming the same mean, x_o, to have occurred at the center of a modulator discharge cycle to give $t_d(x_o) = t_{do}$; and taking the output to be

$$\overline{y} \equiv h \frac{t_{co} - t_{do}}{t_{co} + t_{do}}. \tag{19}$$

This is plausible in view of the asynchronous operation of the modulator. It will then be shown that (19) remains unchanged when the output is defined more rigorously as the average of y(t) over a complete cycle, and x_o is taken as the input mean over the complete cycle.

Consider an input ramp x(t), with mean x_o and slope x' during the feedback charge

cycle. The resulting exponential window waveform is plotted in Fig. XXV-5. The switching limits plotted are the loci of $y_i(t) = -x(t) + w$ and $y_i(t) = -x(t) - w$; the

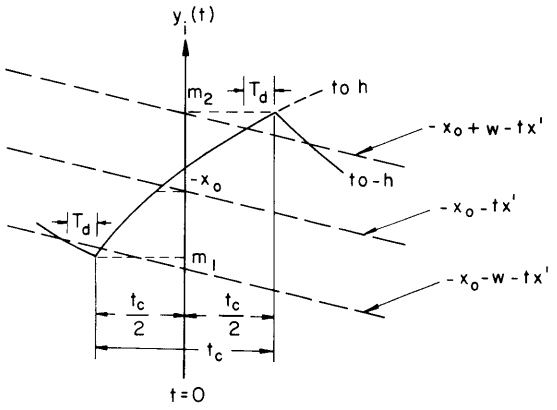

Fig. XXV-5. Intermediate waveform, ramp input.

overshoot occurs because of the delay T_d. From Fig. XXV-5,

$$m_1 = -h + \left[h - x_o - w + x'\left(\frac{t_{co}}{2} + T_d\right)\right] e^{-T_d/\tau} \tag{20}$$

$$m_2 = h + \left[-h - x_o + w - x'\left(\frac{t_{co}}{2} + T_d\right)\right] e^{-T_d/\tau}. \tag{21}$$

Therefore

$$d = \frac{m_2 - m_1}{2} = h\left(1 - e^{-T_d/\tau}\right) + w\, e^{-T_d/\tau} - \frac{x'}{2} e^{-T_d/\tau} t_{co} \tag{22}$$

$$-x_m = \frac{m_1 + m_2}{2} = -(x_o - x'T_d)\, e^{-T_d/\tau}. \tag{23}$$

Similar values of d and x_m are obtained by regarding x_o as the mean of the input ramp during a discharge cycle.

The problem is that d is expressed as a function of t_{co}, hence (22) and (23) cannot be plugged directly into (9) to obtain an explicit expression for $\overline{y}$.

Recall that (9) arose from the expression

$$t_{co} = \tau \ln \frac{h + x_m + d}{h + x_m - d}. \tag{24}$$

Or, to second order, since $\ln\left[\frac{a+\epsilon}{a-\epsilon}\right] = 2\left[\frac{\epsilon}{a} + \frac{1}{3}\left(\frac{\epsilon}{a}\right)^3 + \ldots\right]$,

$$t_{co} = \frac{2\tau d}{h + x_m}. \tag{25}$$

If the implicit expressions for d and x_m are substituted in Eq. 25, we have

$$t_{co} = \frac{2\tau\left[h\left(1-e^{-T_d/\tau}\right)+we^{-T_d/\tau}\right]}{h+\left[x_o-T_dx'\right]e^{-T_d/\tau}} - \frac{\left[\tau x'e^{-T_d/\tau}\right]t_{co}}{h+\left[x_o-T_dx'\right]e^{-T_d/\tau}}. \tag{26}$$

Iterative substitution for t_{co} yields a ratio series

$$t_{co} = \frac{2\tau\left[h\left(1-e^{-T_d/\tau}\right)+we^{-T_d/\tau}\right]}{h+\left[x_o-T_dx'\right]e^{-T_d/\tau}}\left[\frac{1}{1+\dfrac{\tau x'e^{-T_d/\tau}}{h+\left[x_o-T_dx'\right]e^{-T_d/\tau}}}\right] \tag{27}$$

or

$$t_{co} = \frac{2\tau\left[h\left(1-e^{-T_d/\tau}\right)+we^{-T_d/\tau}\right]}{h+\left[x_o+(\tau-T_d)x'\right]e^{-T_d/\tau}}. \tag{28}$$

Comparison of Eq. 28 and Eq. 25 enables identification of equivalent midpoint and half-widths, denoted x_e and d_e, in explicit form:

$$x_e = \left[x_o+(\tau-T_d)x'\right]e^{-T_d/\tau} \tag{29}$$

$$d_e = \left[h\left(1-e^{-T_d/\tau}\right)+we^{-T_d/\tau}\right]. \tag{30}$$

Now equations (29) and (30) may be substituted in Eq. (9) to give the desired transfer function.

$$\boxed{\bar{y} = -\left[x_o+(\tau-T_d)x'\right]e^{-T_d/\tau}\left\{1+\frac{\left[\left(1-e^{-T_d/\tau}\right)+\frac{w}{h}e^{-T_d/\tau}\right]^2}{1-\left[\frac{\left[x_o+(\tau-T_d)x'\right]e^{-T_d/\tau}}{h}\right]^2}\right\}} \tag{31}$$

It will be demonstrated next that (31) remains valid if a complete modulator cycle is considered, with output $\bar{y} = h\dfrac{t_c - t_d}{t_c + t_d}$ and input mean x_o over the complete cycle. The input mean during t_c, from Fig. XXV-6, is

$$x_{oc} = x_o - \frac{t_d}{2} x'. \tag{32}$$

And, during t_d the input mean is

$$x_{od} = x_o + \frac{t_c}{2} x'. \tag{33}$$

Rewriting (28) in terms of the charge and discharge means yields

$$t_c = \frac{2\tau d_e}{h + \left[x_o + (\tau - T_d) x'\right] e^{-T_d/\tau} - \frac{t_d}{2} x' e^{-T_d/\tau}} \tag{34}$$

$$t_d = \frac{2\tau d_e}{h - \left[x_o + (\tau - T_d) x'\right] e^{-T_d/\tau} - \frac{t_c}{2} x' e^{-T_d/\tau}}. \tag{35}$$

Recalling that t_{co} was defined as the charge period with input mean x_o, and t_{do}

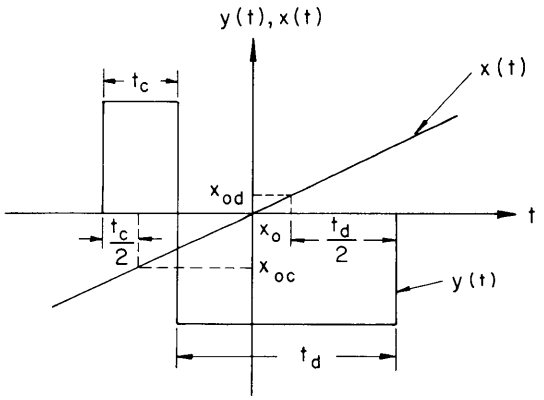

Fig. XXV-6. Complete modulator cycle, ramp input.

as the discharge period with input mean x_o, we can rewrite (34) and (35) as

$$t_c = t_{co} \frac{1}{1 - t_{co} \frac{x' e^{-T_d/\tau}}{4\tau d_e} t_d} \tag{36}$$

$$t_d = t_{do} \frac{1}{1 - t_{do} \frac{x' e^{-T_d/\tau}}{4\tau d_e} t_c}. \tag{37}$$

By identifying $\frac{x' e^{-T_d/\tau}}{4\tau d_e} = A$, iterative substitution gives

$$t_c = t_{co} \cfrac{1}{1 - At_{co}t_{do} \cfrac{1}{1 - At_{co}t_{do} \cfrac{1}{1 - At_{co}t_{do} \cfrac{}{\ddots}}}} \tag{38}$$

$$t_d = t_{do} \cfrac{1}{1 - At_{co}t_{do} \cfrac{1}{1 - At_{co}t_{do} \cfrac{}{\ddots}}} \tag{39}$$

It is sufficient to note that

$$t_c = Bt_{co} \tag{40}$$

$$t_d = Bt_{do}. \tag{41}$$

Whence

$$\overline{y} = h\frac{t_c - t_d}{t_c + t_d} = h\frac{Bt_{co} - Bt_{do}}{Bt_{co} + Bt_{do}} = h\frac{t_{co} - t_{do}}{t_{co} + t_{do}}. \tag{42}$$

This is the desired proof that the output average over a full cycle in terms of the input mean x_o during this cycle is the same as that obtained by superposition of the charge-cycle and discharge-cycle results, each taken separately to have input mean x_o.

It should be pointed out that most of the transfer functions obtained here can also be obtained by direct brute-force algebraic expansion and approximation methods on the transfer function obtained by Bose. Indeed, it was not until direct algebra and computer evaluation had predicted the form of the result that the procedure described in this report was developed. The exponential window technique presented here is, however, simpler to apply, more intuitive, and yields results of a higher order of accuracy than could be obtained by using direct methods and a finite quantity of paper.

A computer program has been written to check the accuracy of the transfer function given by Eq. 31. For a given set of parameter values, the result predicted by (31) is compared with the exact output found by numerical analysis methods. Results of the program will be outlined in greater detail at a later date; however, it will be mentioned here that over a wide range of parameters the error in (31) is typically less than 0.2 per cent of the modulator hysteresis height. Even for the rather poor operating values of $h = 1$, $\frac{w}{h} = 0.05$, $T_d/\tau = 0.05$, $\frac{\tau x'}{h} = 0.2$ and $x_o = 0.95$, the output

predicted by (31) is only 0.006 higher than the exact result, $\overline{y} = 0.716$.

The exponential window approach can be applied to evaluate a broader class of systems than the two-state modulator. For example, the response of a bang-bang servomechanism can be effectively characterized by utilizing this technique.

J. E. Schindall

References

1. A. G. Bose, Quarterly Progress Report No. 66, Research Laboratory of Electronics, M.I.T., July 15, 1962, pp. 187-189.
2. A. G. Bose, Quarterly Progress Report No. 67, Research Laboratory of Electronics, M.I.T., October 15, 1962, pp. 115-119.

B. A NEW APPROACH TO ECHO REMOVAL

In many situations one is faced with the problem of processing signals that have been combined by convolution. Such signals occur in high-fidelity recording, sonar, multipath communication channels, and seismology. In general, the problem is one of extraction of one signal from the convolution of two or more. For example, if a signal s(t) is passed through an environment that introduces echoes, the result is a signal x(t) of the form

$$x(t) = s(t) + \alpha s(t-t_o). \tag{1}$$

This signal can be thought of as the convolution of s(t) with an impulse train as in Eq. 2a and Eq. 2b.

$$x(t) = s(t) \otimes u_\alpha(t) \tag{2a}$$

$$u_\alpha(t) = u_o(t) + \alpha u_o(t-t_o). \tag{2b}$$

If the signal s(t) is to be recovered, the impulse train must be removed. Alternatively, if only information regarding the presence and the timing of the echo is required, it might be desirable to remove the signal s(t) and recover only the impulses.

The system shown in Fig. XXV-7 has been proposed for the purpose of separating convolved signals.[1] It has been shown[2,3] that such a system is a member of a larger class of nonlinear systems called homomorphic systems which obey a generalized principle of superposition. In Fig. XXV-7a, the system L is a linear system obeying superposition in the conventional sense, and the system $A_\otimes$ is specified by Fig. XXV-7b, where X(f) is the Fourier transform of x(t), and

$$\hat{X}(f) = \log X(f).$$

The system $A_\otimes^{-1}$ is simply the inverse of $A_\otimes$. From the definition of $A_\otimes$, it can be

shown that if

$$x(t) = x_1(t) \otimes x_2(t),$$

then

$$\hat{x}(t) = \hat{x}_1(t) + \hat{x}_2(t). \tag{3}$$

In this report, some results pertaining to the removal of echoes, by using the system of Fig. XXV-7a, will be given and an example will be discussed.

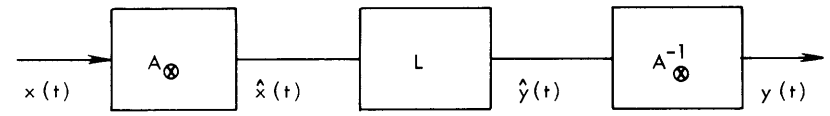

(a)

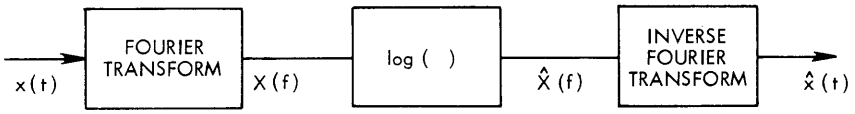

(b)

Fig. XXV-7. (a) Canonic form for convolution filter.
(b) Realization of the system $A_{\otimes}$.

In order to understand how to choose the linear system L in any filtering application, it is necessary to characterize the signals that will be present at the output of system $A_{\otimes}$. Some results will be given without proof for some typical signals that arise in the removal of echoes from speech signals. Following the presentation of these results, is a discussion of their application.

1. Echoes

Equation 2 shows the form of a signal with a single echo of amplitude α and delay t_o. From Eq. 3, it is seen that

$$\hat{x}(t) = \hat{s}(t) + \hat{u}_{\alpha}(t). \tag{4}$$

The signal $\hat{u}_{\alpha}(t)$ can be shown to be

$$\hat{u}_{\alpha}(t) = \sum_{n=1}^{\infty} (-1)^{n+1} \frac{\alpha^n}{n} u_o(t-nt_o) \qquad \text{if } \alpha < 1. \tag{5}$$

2. Aperiodic Waveforms

General results are not known about the response of system $A_{\otimes}$ to an arbitrary waveform. For an aperiodic function p(t), which is zero for $t < 0$ and has a Fourier transform that is a rational function of $j2\pi f$, however, something can be said about the response p(t) for $t > 0$.

It is found, that for $t > 0$, the output of system $A_{\otimes}$ is of the form

$$\hat{p}(t) = \frac{-1}{j2\pi t} \int_{-\infty}^{\infty} \frac{P'(f)}{P(f)} e^{j2\pi ft}\, df, \tag{6}$$

where P(f) is the Fourier transform of the input p(t). From Eq. 6, it can be shown that if the transform of the input has all its poles and zeros in the left half-plane, then

$$|\hat{p}(t)| \leq A \frac{e^{-bt}}{t} \qquad t > 0, \tag{7}$$

where A and b are positive constants, and -b is greater than the real parts of all the poles and zeros of the transform of p(t). This means simply that although p(t) goes to zero exponentially, $\hat{p}(t)$ will go to zero even faster.

3. Periodic Signals

Consider a signal x(t) of the form

$$x(t) = \sum_{m=0}^{M-1} p(t-mT). \tag{8}$$

Equation 8 could be rewritten

$$x(t) = p(t) \otimes u(t) \tag{9a}$$

$$u(t) = \sum_{m=0}^{M-1} u_o(t-mT). \tag{9b}$$

Such a signal could represent a segment of a speech waveform during an interval corresponding to a voiced sound. In this case, p(t) would be an exponentially decaying aperiodic function, and T would correspond to the pitch period. The response of system $A_{\otimes}$ to the input of Eq. 8 is

$$\hat{x}(t) = \hat{p}(t) + \hat{u}(t), \tag{10}$$

where $\hat{u}(t)$ can be shown to be

$$\hat{u}(t) = \sum_{n=1}^{\infty} \frac{1}{n} u_o(t-nT) - \sum_{n=1}^{\infty} \frac{1}{n} u_o(t-nMT). \tag{11}$$

The output of system $A_{\otimes}$ thus consists of the sum of a signal $\hat{p}(t)$, which is going to zero as in Eq. 7, and two impulse trains for which the areas approach zero as $\frac{1}{n}$ and whose spacings are T and MT.

4. Exponential Weighting of Inputs

Suppose the input given by Eq. 8 is multiplied by an exponential to give

$$x_1(t) = e^{-at} x(t).$$

This expression can be rewritten

$$x_1(t) = \sum_{m=0}^{M-1} p_1(t-mT)\, e^{-amT},$$

where

$$p_1(t) = e^{-at} p(t).$$

The output of system $A_{\otimes}$ then becomes

$$\hat{x}_1(t) = \hat{p}_1(t) + \sum_{n=1}^{\infty} \frac{e^{-anT}}{n} u_o(t-nT) - \sum_{n=1}^{\infty} \frac{e^{-anMT}}{n} u_o(t-nMT). \tag{12}$$

In a similar way, it can be shown that the effect of exponentially weighting an input containing echoes (Eq. 1) is to produce the output

$$\hat{x}_1(t) = \hat{s}_1(t) + \sum_{n=1}^{\infty} (-1)^{n+1} \frac{\alpha^n e^{-ant_o}}{n} u_o(t-nt_o) \tag{13}$$

where $\hat{s}_1(t)$ is the response to $s_1(t) = e^{-at} s(t)$.

It can be seen from the results just presented that the effect of system $A_{\otimes}$ is to tend to produce outputs that occupy different regions of time. In general, aperiodic pulse-type waveforms produce outputs that approach zero after a very short time, while impulse trains of finite duration produce impulse trains of infinite duration that go to

zero at least as fast as $\frac{1}{n}$. This suggests that in some situations, the outputs will occupy different intervals of time so that a "frequency-invariant"[1] linear filter should be used for system L in Fig. XXV-7a. For example, if x(t) is a speech signal with an echo

$$x(t) = s(t) \otimes u_a(t) \tag{14a}$$

$$s(t) = p(t) \otimes u(t), \tag{14b}$$

x(t) is the convolution of three signals and the response of the system $A_{\otimes}$ will be the sum of the corresponding responses to these three inputs

$$\hat{x}(t) = \hat{p}(t) + \hat{u}_a(t) + \hat{u}(t). \tag{15}$$

If $T \ll t_o$, the three components of the response essentially occupy different time intervals, as can be seen from Eqs. 7, 5 and 11. For example, if the echo is to be removed, a "frequency-invariant comb filter," as shown in Fig. XXV-8, could be used. In using

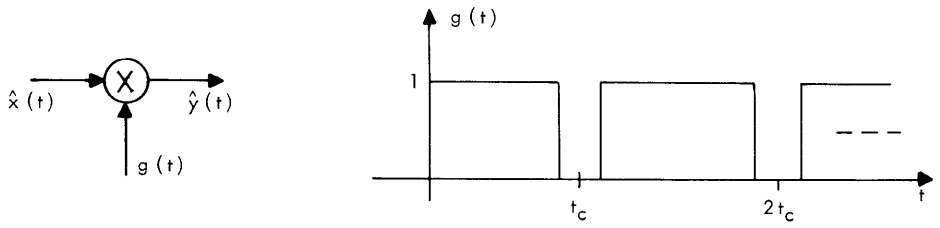

Fig. XXV-8. Ideal frequency-invariant filter for echo removal.

such a system it is clear that the echo timing need not to be known exactly but must only fall in the region around t_c.

It should be pointed out that for speech signals the character of the waveform changes as time increases, so that it is neither possible nor desirable to perform a Fourier transformation of a speech signal of long duration, even if the complete waveform is available (e.g., a recording). For this reason, the Fourier transformation indicated in Fig. XXV-7b should be replaced by a "short-time" Fourier transform defined as

$$X(f,t) = \int_{-\infty}^{\infty} w(t-\tau)\, x(\tau)\, e^{-j2\pi f\tau}\, d\tau. \tag{16}$$

In Eq. 16, $w(\tau)$ is a "window" function of finite duration. Such an operation on the signal $x(\tau)$ can be interpreted as a Fourier transformation of $x(\tau)$ when viewed through a

window that slides along as t increases.

It should be clear that the logarithmic operation in Fig. XXV-7a takes advantage of the fact that if two signals are convolved, their transforms are multiplied. For a short-time transform of Eq. 1, it can be shown that

$$X(f,t) = S(f,t) + \alpha S(f,t-t_o)\, e^{-j2\pi f t_o}.$$

If S(f,t) does not change too rapidly as t changes, we can see that in some sense

$$X(f,t) \approx S(f,t)\left[1+\alpha\, e^{-j2\pi f t_o}\right]. \tag{17}$$

Therefore taking the logarithm of X(f,t) produces approximately the same behavior as before. Intuitively, the requirement that the approximation of Eq. 17 hold is equivalent to requiring that the window be wide compared with the echo time t_o.

Whether a short-time transform is required or not, it is necessary to give some attention to the computational aspects of realizing the system of Fig. XXV-7. A system of this type has been programmed for the PDP-1 computer and has been used to obtain results that are consistent with the previous discussion. The Fourier analysis is done by using the Cooley-Tukey algorithm[4] for evaluating the equations

$$X(k) = \sum_{t=0}^{N-1} x(t)\, e^{-j\frac{2\pi}{N}kt} \qquad k = 0, 1, \ldots, N-1 \tag{18a}$$

$$x(t) = \frac{1}{N}\sum_{k=0}^{N-1} X(k)\, e^{j\frac{2\pi}{N}kt} \qquad t = 0, 1, \ldots, N-1. \tag{18b}$$

The results for the response of system $A_{\otimes}$ given in the previous equations assume that time and frequency are continuous variables. All of these results have their counterparts in the case for which time and frequency are discrete as in Eqs. 18a and 18b. There are two major differences. First, unit impulses are replaced by unit samples. Second, because of the sampled nature of the time function and the frequency function, Eqs. 18a and 18b are actually periodic with period N. This means, for example, that in the infinite sum in Eq. 5 all values of nt_o must be taken mod N. Therefore a unit sample of height $\frac{\alpha^n}{n}(-1)^{n+1}$, which is supposed to occur at $t = nt_o$ with $2N > nt_o > N$, will actually occur at $(nt_o - N)$. This aliasing effect is minimized computationally by exponential weighting of the input, since it is clear from Eq. 13 that the corresponding weighted sample has height $(-1)^{n+1}\frac{\alpha^n}{n}e^{-ant_o}$.

As an example of the type of processing that is proposed, consider Fig. XXV-9. Figure XXV-9a shows a section of the vowel "ah" which has an echo at t_o = 300 samples

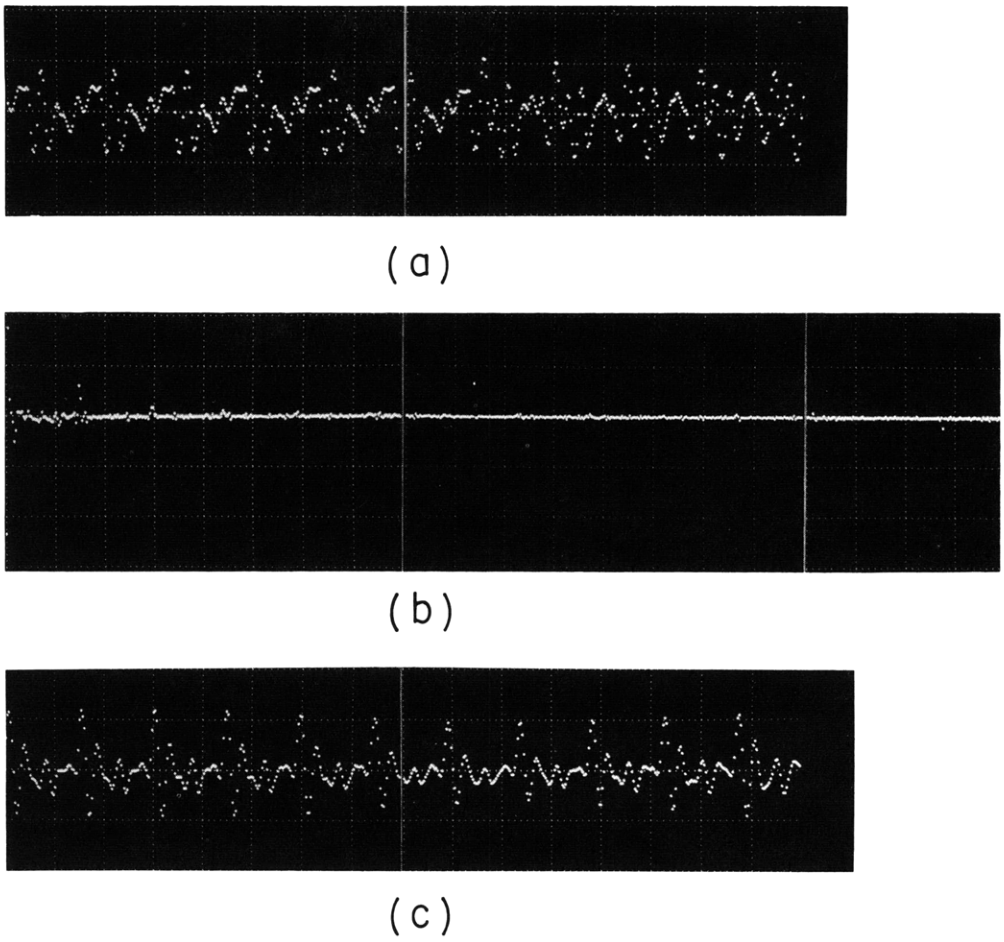

Fig. XXV-9. (a) Segment of the vowel "ah" with an echo at 300 samples.
(b) Output of the system $A_{\otimes}$ for the exponentially weighted input of (a).
(c) Output of system after the removal of echo.

(sampling rate of 10 kHz). Figure XXV-9b shows the corresponding output of system $A_{\otimes}$ for the exponentially weighted input. The peaks at t = 300 and 600 are due to the echo, and the peaks at multiples of 46 (the pitch period) are due to the middle term in Eq. 12. The points that are due to p(t) are seen to be essentially limited to the region between 0 and 46. The peaks predicted by the last term in Eq. 12 do not appear because MT is greater than N and e^{-aMT} is very small. The waveform of Fig. XXV-9c shows the

output of the system of Fig. XXV-7a when the linear system L is a frequency-invariant filter with g(t), as shown in Fig. XXV-8.

Many theoretical and computational problems remain to be resolved. The ideas and results reported here do seem to hold promise of application in a wide variety of waveform-processing situations.

R. W. Schafer

References

1. A. V. Oppenheim, "Nonlinear Filtering of Convolved Signals," Quarterly Progress Report No, 80, Research Laboratory of Electronics, M.I.T., January 15, 1966, pp. 168-175.
2. A. V. Oppenheim, "Superposition in a Class of Nonlinear Systems," Technical Report 432, Research Laboratory of Electronics, Massachusetts Institute of Technology, Cambridge, Massachusetts, March 31, 1965.
3. A. V. Oppenheim, "Optimum Homomorphic Filters," Quarterly Progress Report No. 77, Research Laboratory of Electronics, M.I.T., April 15, 1965, pp. 248-260.
4. J. W. Cooley and J. W. Tukey, "An Algorithm for the Machine Calculation of Complex Fourier Series," Mathematics of Computation, Vol. 19, pp. 297-301, April 1965.